

五 院

○五四系



序号	姓 名	职 称	单位	论 文 题 目	刊物、会议名称	年、卷、期	类别
1	陈静勇 周来水	硕士 正高	054 054	基于Java3D的虚拟现实建模方法	计算机应用研究	2002.19.05	J
2	陈俊 周来水	硕士 正高	054 054	一种基于Web的CAD/CAM系统 开发方案	机械设计与制造工程	2002.31.01	J
3	陈明和 高霖 周建华 王琨	副高 正高 副高 正高	054 054 054 054	Application of reaction sintering to the manufacturing of a spacecraft combustion chamber of Sic ceramics	Juornal of Materials Processing Technology	2002.129.1-3	SCI、 W
4	程筱胜 沈建新	副高 中级	054 054	PDM与图档管理的异同	机械制造与自动化	2002.00.05	
5	崔耀东 周儒荣 廖文和	博士 正高 正高	054 054 054	制造业信息技术应用之间的协同 效应分析方法	机械科学与技术	2002.21.03	H
6	崔耀东 周儒荣 廖文和	博士 正高 正高	054 054 054	考虑协同效应时制造业信息系统 应用水平的评价方法	信息与控制	2002.31.01	H
7	崔耀东 周儒荣	博士 正高	054 054	Generating optimal cutting Patterns for rectangular blanks of a single size	Journal of the Operational Research Society	2002.53.12	SCI、 W
8	董洪伟 周儒荣 周来水	博士 正高 正高	054 054 054	在ACIS几何平台上开发三维软件	计算机辅助工程	2002.11.04	J
9	冯雪飞 陈文亮	硕士 副高	054 054	Windows平台下串行通信的几种 实现方法	机械制造与自动化	2002.00.01	
10	高霖	正高	054	Classification and analysis of tube htdroforming processes with respect to adaptive FEM simulations	J.Materials Processing Technology	2002.129.00	SCI、 W
11	侯继英 曾建江 陈文亮	硕士 中级 副高	054 011 054	全球制造中图样的自动转换方法	机械设计与制造工程	2002.31.01	J
12	黄翔 张社教 刘光辉 曾荣	副高 其他1 硕士 中级	054 054 054 054	CAD应用标准化工作的研究	计算机集成制造系统	2002.18.10	J
13	黄翔 阎崇京	副高 硕士	054 054	跨零件特征造型技术的研究	第一届全国几何设计与计 算学术	2002.01	
14	黄翔	副高	054	CAD、艺术、设计与教育	南京航空航天大学学报社 科版	2002.04.18	
15	黄翔 曾荣 岳伏军 廖文和	副高 中级 其他1 正高	054 054 外 054	NURBS插补技术在高速加工中的 应用研究	南京航空航天大学学报	2002.34.01	J

序号	姓 名	职 称	单位	论 文 题 目	刊物、会议名称	年、卷、期	类别
16	黄翔 阎崇京	副高 硕士	054 054	Research on Knowledge-based Connecting Elements Modeling	Journal of Ximen University	2002.13.18	H
17	黄翔 葛友华 曾荣 廖文和	副高 硕士 中级 正高	054 054 054 054	基于WEB的智能CAPP系统的研究	中国机械工程	2002.13.10	H
18	黄翔 阎崇京	副高 硕士	054 054	机械联接单元快速造型方法的研究	中国机械工程	2002.13.18	H
19	金修宝 陈文亮 张胜 翟建军	硕士 副高 硕士 副高	054 054 054 054	有限元网格孔洞的自动填充算法	机械制造与自动化	2002.00.06	
20	刘长毅 徐诚 廖文和	中级 其他1 正高	054 054 054	CBD中实例参数调整的诊断与判 别	计算机应用	2002.22.09	J
21	刘浩 唐月红	博士 副高	054 054	NURBS曲面间的最短距离	南京理工大学学报	2002.26.04	J
22	鲁世红 恽君璧	副高 副高	054 054	Theoretical model of the transformation Superplastic diffusion bonding of eutectoid Steel	Journal of Materials Processing Technology	2002.129.10	SCI、 W
23	鲁世红 恽君璧	副高 副高	054 054	具有柔性滚轴的两轴卷筒机研制	锻压机械	2002.37.01	J
24	鲁世红 恽君璧	副高 副高	054 054	The retical Model of Transformation Superplastic Diffusion Bonding for Eutectoid Steel	厦门大学学报	2002.41.增刊	H
25	倪卫华 曾建江 陈文亮	硕士 中级 副高	054 011 054	基于特征参数化的工艺设计方法	机械制造与自动化	2002.00.01	
26	沈建新	中级	054	准分子激光切削角膜的数学模型 与切削技术	第八届全国激光生物学学 术会议	2002.01	
27	沈建新	中级	054	中小企业电子商务的关键技术	机械制造与自动化	2002.00.05	
28	沈建新	中级	054	CAPP特征推理技术与实现	第二届全国先进制造技术	2002.01	
29	沈建新	中级	054	数控加工中参数线刀具轨迹生产 方法的研究	计算机辅助设计与制造	2002.00.01	
30	沈建新	中级	054	动态规划模型在生产库存优化中 的应用研究	机械设计与制造工程	2002.31.11	J

序号	姓 名	职 称	单位	论 文 题 目	刊物、会议名称	年、卷、期	类别
31	童国权 高霖 林兆荣	副高 正高 正高	054 054 054	The Grain Size Dependency of Compressive Deformation of a superplastic 3mol% Yttria Stabilized Tetragonal Zirconia	Material Science and Engineering A	2002.A336.01	SCI、W
32	王占东 周来水 张丽艳	博士 正高 副高	054 054 054	基于Doo/Sabin细分的分片光滑曲面重建算法研究	机械设计与制造工程	2002.31.06	J
33	徐啸峰 周儒荣 安鲁陵 周来水	博士 正高 副高 正高	054 054 054 054	基于ACIS几何平台的两维数控加工编程技术研究	机械科学与技术	2002.21.01	H
34	徐啸峰 周儒荣 周来水	博士 正高 正高	054 054 054	产品特征间关系的表达和算法研究	南京航空航天大学学报	2002.34.06	J
35	徐啸峰 周儒荣 周来水	博士 正高 正高	054 054 054	智能CAD的产品设计知识研究	计算机辅助工程	2002.11.03	J
36	许海马 张丽艳 庄海军	硕士 副高 中级	054 054 054	轴类零件自动化分布式CAX集成系统的研究与实践	机械科学与技术	2002.21.05	H
37	薛建勋 周来水	硕士 正高	054 054	基于Web的CAD/CAM系统设计与关键技术研究	制造业自动化	2002.24.增刊	J
38	阎崇京 黄翔	硕士 副高	054 054	零件信息模型的研究与应用	机械设计与制造工程	2002.31.05	J
39	曾荣 廖文和 马驰容	中级 正高 硕士	054 054 054	基于组件的分布式CAPP系统的体系结构研究	机械设计与制造工程	2002.31.06	J
40	曾荣	中级	054	制造业信息编码技术的研究	成组技术与生产现代化	2002.19.04	
41	曾荣 费春涌 晏志军	中级 其他2 其他2	054 054 054	工艺规程编辑器的研究与开发	机械制造与自动化	2002.00.02	
42	曾荣 田宏 黄翔	中级 其他2 副高	054 054 054	现代远程教育系统平台的构造	南京航空航天大学学报社科版	2002.04.18	
43	张丽艳 周儒荣 朱剑英 吴熹	副高 正高 正高 硕士	054 054 053 053	Piecewise B-Spline surfaces fitting to arbitrary triangle meshes	Annals of the CIRP	2002.52.01	SCI、W
44	张丽艳 周来水 蔡炜斌 周儒荣	副高 正高 硕士 正高	054 054 054 054	基于截面测量数据的B样条曲面重建	应用科学学报	2002.20.03	H
45	张丽艳 潘小林 安鲁陵	副高 硕士 副高	054 054 054	网格曲面中孔洞的光滑填充算法研究	工程图学学报	2002.00.04	J

序号	姓 名	职 称	单 位	论 文 题 目	刊物、会议名称	年、卷、期	类别
46	张丽艳 聂军洪 周来水 周儒荣	副高 博士 正高 正高	054 054 054 054	自适应三角网格模型重新布点算法研究	计算机辅助设计与图形学学报	2002.14.03	EI、H
47	张丽艳 周儒荣 唐杰 周来水	副高 正高 博士 正高	054 054 054 054	带属性三角网格模型简化算法研究	计算机辅助设计与图形学学报	2002.14.03	EI、H
48	张丽艳 安鲁陵 王占东 周来水	副高 副高 博士 正高	054 054 054 054	基于人工布点规划的测量数据模型重建	机械科学与技术	2002.21.02	H
49	张丽艳 周儒荣 周来水	副高 正高 正高	054 054 054	三角网格模型中孔洞修补算法研究	应用科学学报	2002.20.02	H
50	张永康 黄翔	硕士 副高	054 054	基于特征的工艺生成方法的研究	机械制造与自动化	2002.00.04	
51	周海 周来水	博士 正高	054 054	单晶 α -Al ₂ O ₃ 镜面加工工艺研究	天津大学学报	2002.35.01	H
52	庄海军 周儒荣 唐杰 张丽艳 周来水	中级 正高 博士 副高 正高	054 054 054 054 054	NURBS曲线在快速原型制造系统中的应用	机械科学与技术	2002.21.06	H
53	庄海军 周儒荣 安鲁陵 周来水	博士 正高 副高 正高	054 054 054 054	一种基于实体模型的三轴数控加工刀轨生成算法	南京航空航天大学学报	2002.34.04	J

文章编号:1005-2615(2002)04-0332-04

一种基于实体模型的三轴数控加工刀轨生成算法

庄海军 周儒荣 安鲁陵 周来水

(南京航空航天大学机电学院 南京,210016)

摘要 实体模型是几何造型的高级模型,它具有完整的曲面拓扑关系。国内基于实体模型的数控加工算法的需求日渐迫切,本文提出了一种适合实体模型的三轴数控加工刀位轨迹生成算法:首先根据加工行距作一组平行于刀轴的平面,与模型的待加工表面求交,得到一系列交线;再根据加工步长规划另一组与上述平面垂直且平行于刀轴的平面,与上述交线求交,得到一交点网格,判断刀具与数据点的位置关系从而得到刀位轨迹。

关键词:CAD/CAM;数控加工编程;实体模型

中图分类号:TP391

文献标识码:A

引言

实体模型是几何造型的高级模型,它可提供三维形体的最完整的几何和拓扑信息。从技术发展的趋势看,它在CAD/CAM中的重要性将越来越大。在计算机集成制造的环境下,需要将产品的有关设计制造管理信息尽量完整地包含在数字化定义中,以便提高生产过程中各个环节的自动化和智能化处理水平。使用实体模型将有助于推动设计工作中自动推理机制的运用,提高成组技术的应用水平,实现数控加工刀具轨迹的自动生成和校验加工过程的动态仿真和干涉检查,因此有着广阔的发展和应用前景^[1]。

自20世纪60年代末期各国研究工作者为建立实体模型进行了长期深入的理论研究和试验探讨,实体造型技术已经成熟并已应用到国外商品化CAD/CAM系统中。国外很多软件厂商推出了基于实体造型技术的CAD/CAM平台,基于商业利益的考虑,国外基于实体的数控加工算法虽已成熟,但有关文章很少发表,国内更很少有人从事这方面的研究。

为了尽快赶超国际先进水平,打破国外CAD/CAM商品化软件对我国软件市场的垄断,作者所在单位正应用ACIS几何平台,力图从高起点进行新一代CAD/CAM系统的开发。ACIS是Spatial Technology公司的产品,采用B-rep表示方法定义实体。作者在开发实践过程中,提出了一种基于实体模型的三轴数控加工刀位轨迹生成算法,该算法已在“超人2000 CAD/CAM”系统中实现并应用到实际生产中。

1 基于实体模型的数控加工算法概述

1.1 单元切削法

文[2]提出一种基于八叉树分割的单元切削法,其基本思想是:根据八叉树实体造型方法,将毛坯体均匀分割成八个三维立方体,然后判断每个立方体与待加工表面和毛坯的上表面所形成的加工区域之间的关系。一般有以下三种情况:

(1)立方体完全位于加工区域外部,记为空立方体;

(2)立方体完全位于加工区域内部,记为满立

基金项目:国家“九五”重点科技攻关专题(编号:96-A01-01-05)和江苏省“九五”重大科技攻关(编号:G98017-3)资助项目。

收稿日期:2001-08-27; **修订日期**:2001-10-18

作者简介:庄海军,男,博士研究生,1970年9月生;周儒荣,男,教授,博士生导师,1935年1月生;安鲁陵,男,副教授,1962年7月生;周来水,男,教授,博士生导师,1962年10月生。

方体;

(3)立方体部分位于加工区域内部,与待加工曲面相交,记为部分立方体。

满立方体和空立方体无需再分割,而部分立方体则要继续分割,再分为更小的空立方体和满立方体,直到满足加工精度为止。此时,满立方体的集合即为要切除的区域,每个满立方体可以看作是一个加工单元。将具有相同高度的满立方体重新组织排序,即可生成刀具轨迹。单元切削法适合基于八叉树方法的实体造型系统,这是因为在造型阶段零件已被表示成八叉树形式,但不适于其他造型系统。

1.2 网格高度法

文[3]认为零件加工刀轨主要依赖于零件的数学描述,因而不必通过分割来求得刀轨,他们提出了网格高度法,其基本思想是将B-rep实体模型转化为网格模型,三维零件实体用记录网格高度的二维数组表示,通过网格高度数组生成刀具轨迹。过程大致如下:

(1)将B-rep实体模型中的待加工曲面投影到 xoy 平面上(假设刀具轴线平行于 z 轴),找出投影区域的最大包围盒(长方形),根据用户给定的网格大小,将包围盒划分成 n 行 m 列,共 $n \times m$ 个长方形小网格;

(2)对每一个长方形的小网格,过其中的一个顶点作平行于 z 轴的直线,与每一张待加工曲面求交,找出所有交点中最大的 z 坐标值作为该顶点的高度值,依次求出其他顶点的高度值,将四个顶点中的最大高度值作为该小网格的高度值;

(3)当小网格区域内部点的 z 坐标值大于小网格四个顶点的高度值时,修改小网格的高度值。将所有的网格高度值存放在 n 行 m 列二维数组中;

(4)在每一等高面上,根据网格高度值的二维数组,生成刀具轨迹。

网格高度法在修改网格的高度值时,利用曲面的显式表达式求曲面在小网格区域内的极大值。但曲面一般用参数形式表达,很难表示为显式表达式,因而网格高度法在实际使用时受到很大的限制。

2 算法思想

针对上述算法存在的不足之处,作者提出采用Z-buffer理论生成实体模型的无干涉刀位轨迹,具

体思路是:设刀轴方向为 z 轴方向,将实体模型的加工表面描述成 xoy 平面上的 z 向单值函数,工件的加工表面被相距分别为 S_1 和 S_2 的平行于 xoz 平面和 $yo z$ 平面的平面离散成 n 行 m 列数据点,每一数据点用 $\{x(i), y(j), z(i, j)\}$ 表示,其中

$$\begin{cases} z(i, j) = f(x(i), y(j)) \\ x(i) = x_0 + i * S_1 \\ y(j) = y_0 + j * S_2 \end{cases}$$

z 方向的高度值与 xoy 平面的点 (x, y) 存在一一对应的单值函数关系, $z(i, j) = f(x(i), y(j))$ 就代表了被加工零件的形状。数据结构可以采用二维数组的形式,存储为 $z[i][j]$ 的格式,本文叫做Z-buffer模型。

3 Z-buffer模型的生成

实体模型按精度离散一直是人们研究的热点。在无干涉刀具轨迹的生成过程中,经常按精度将加工表面离散成一系列三角片^[4~7],用三角片去近似表示原加工表面,但三角片本身具有很多缺点^[8]。文[3]的方法实际上是把加工表面离散成四边形网格。本文采用如下步骤(如图1所示):

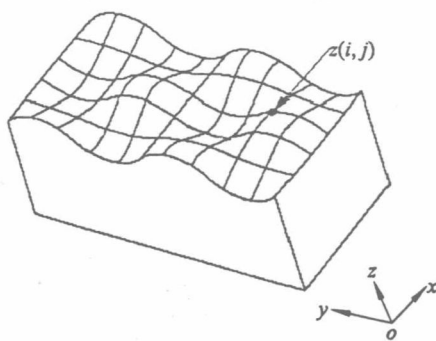


图1 Z-buffer模型的生成示意图

(1)求待加工实体表面在 xoy 平面投影的最大包围盒;

(2)沿 x 方向在包围盒内作平行平面,两相邻平行平面之间的距离 S_1 为用户输入的加工行距。各平行平面分别与待加工于实体表面求交,得一系列交线,记为 x 向交线;

(3)沿 y 方向在包围盒内作平行平面,两相邻平行平面之间的距离 S_2 为用户输入的加工步长。各平行平面分别与 x 向交线求交,若某一平面与同一交线有两个或两个以上的交点,则取 z 值最大的交点,将交点存放在数组中;

由于“超人2000 CAD/CAM”系统是在ACIS几何平台基础上开发的,ACIS提供了稳定的几何

求交函数,为本算法奠定了基础。

4 刀具轨迹的产生

为了叙述方便,本文以圆角刀为例,刀具半径为 R , 刀具圆角半径为 r , 根据 Z-buffer 模型产生刀位轨迹类似于数控加工编程中的投影法^[9~10], 设 $P(m, n) = \{x(m), y(n), z(m, n)\}$ 为 Z-buffer 模型中的一点, 则在此点上方无干涉的刀位点的 z 坐标为

$$z' = \max\{z(i, j) + (h(i, j, m, n; R))\} \quad (1)$$

$$(i, j) \in I(m, n; R)$$

其中

$$\begin{cases} I(m, n; R) = \{(i, j) | (\Delta x_{im}^2 + \Delta y_{jn}^2) \leq R^2\} \\ h(i, j, m, n; R) = \begin{cases} r & q \leq R - r \\ \sqrt{r^2 - (q - R + r)^2} & R - r < q \leq R \end{cases} \\ q = \sqrt{\Delta x_{im}^2 + \Delta y_{jn}^2} \\ \Delta x_{im} = x(m) - x(i) \\ \Delta y_{jn} = y(n) - y(j) \end{cases}$$

式(1)给出了在刀具投影范围内无干涉的刀位点的 z 坐标, $h(i, j, m, n)$ 表示刀触点 $P(i, j)$ 到刀具中心点的高度(见图 2)。连接所有的刀位点,生成刀具轨迹。

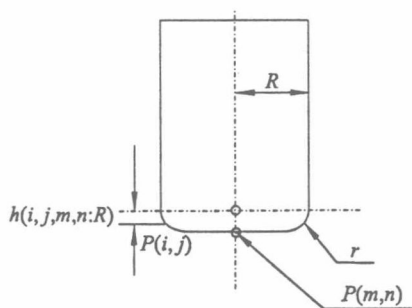


图2 刀具示意图

5 编程实例

作者用 Z-buffer 模型代替被加工零件模型, 使得刀位计算方法变得简便, 算法稳定。本文的算法已在“超人 2000 CAD/CAM”系统中实现。图 3 为实际生产中的一个锻模零件造型, 图 4 为采用本算法产生的刀位轨迹, 图 5 为加工结果。

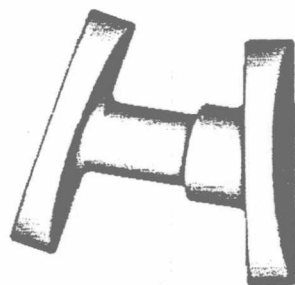


图3 锻模造型

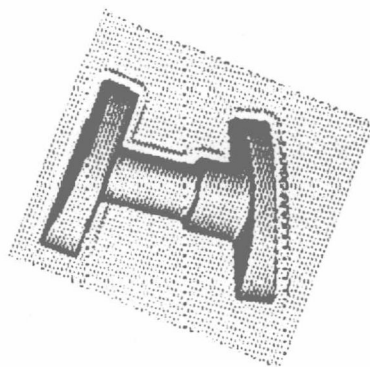


图4 加工刀轨

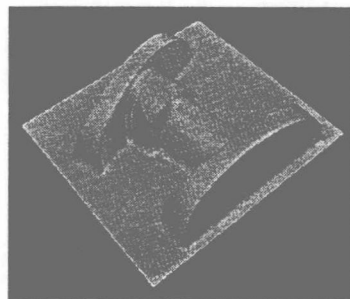


图5 加工结果

6 结 论

本文提出的算法已在南京航空航天大学 CAD/CAM 工程研究中心开发的“超人 CAD/CAM”系统中实现。大量实践表明, 基于实体模型的数控粗加工在计算速度、加工可靠性方面均比基于曲面模型的数控粗加工编程有了较大的提高, 而且在很大程度上简化数控代码的生成过程, 方便了系统使用者, 具有很好的工程实用性。应该说明的是, 本算法仅适用于一般实体模型, 对具有与 z 方向同向的垂直壁的零件的切削轨迹生成问题还有待进一步研究。

参 考 文 献

- 1 唐荣锡. 计算机辅助飞机制造[M]. 北京:航空工业出版社,1993. 169~170
- 2 Lee K, Kim T J, Hong S E. Generation of toolpath with selection of proper tools for rough cutting process[J]. Computer Aided Design, 1994, 26(11): 822~831
- 3 You Chunfong, Chu Chinsing. An automatic path generation method of NC rough cut machining from solid models[J]. Computer in Industry, 1995, 26: 161~173
- 4 Ji Seon Hwang, Chang Tienchien. Three-axis machining of compound surfaces using flat and filleted end-mills[J]. Computer Aided Design, 1998, 30(8): 641~647
- 5 Ji Seon Hwang. Interference-free tool-path generation in the NC machining of parametric compound surface [J]. Computer Aided Design, 1992, 24(12): 667~676
- 6 Li S X, Jerard R B. 5-axis machining of sculptured surface with flat-end cutter[J]. Computer Aided Design, 1994, 26(3): 165~178
- 7 沈庆云, 周儒荣. 参数曲面的拟自适应三角化[J]. 南京航空航天大学学报, 1999, 31(4): 381~387
- 8 唐 杰. 逆向工程中三角网格模型的数据处理技术研究[D]:[学位论文]. 南京航空航天大学, 2000
- 9 Hansen A, Arbab F. Fixed-axis tool positioning with built-in global interference checking for NC path generation[J]. IEEE Journal of Robotics and Automation, 1988, 4(6): 610~621
- 10 冉瑞江. 实用化数控加工编程系统的研究与开发[D]. [学位论文]. 北京:北京航空航天大学, 1994

New Tool Path Generation Algorithm for Three-Axis NC Machining Based on Solid Model

Zhuang Haijun Zhou Rurong An Luling Zhou Laishui

(College of Mechanical and Electrical Engineering,
Nanjing University of Aeronautics & Astronautics Nanjing 210016, P. R. China)

Abstract Solid models possess a complete topological relation of surfaces. An algorithm is used to study tool path generation based on solid models. A NC machining algorithm for generation of tool path based on solid model is presented. Firstly a group of planes parallel to cutter axis are made in terms of row space. A series of intersecting curves are obtained by intersection of the planes with the model to be machined. Then a set of planes perpendicular to the above planes and parallel to cutter axis is built according to machining step length. Using intersection with the above intersecting curves, an intersecting point mesh is generated. These intersecting points are put into a array and the tool path is generated by determining the positional relation of the cutter with these points.

Key words: CAD/CAM; NC programming; solid model

文章编号:1003-8728(2002)06-1001-03



庄海军

NURBS 曲线在快速原型制造系统中的应用

庄海军,周儒荣,唐 杰,张丽艳,周来水

(南京航空航天大学 CAD/CAM 工程研究中心,南京 210016)

摘 要:大多数快速原型制造系统采用 STL 文件作为与 CAD 系统之间的数据交换接口。但是,STL 文件是通过用一系列的三角片逼近实际零件表面而产生的,STL 文件本身及其创建过程均存在许多问题。要提高模型的精度,就必须增加三角片的数量,同时减小三角片的尺寸。这必然造成 STL 文件庞大,后续处理时间较长,而且易产生缺陷,使后续处理不能进行。针对上述问题,本文分析了 STL 文件的不足,提出一种 CAD 系统与 RPM 系统之间新的数据交换方法。该方法对 CAD 系统中的真实模型直接切片,将切片后所得到的轮廓数据作为 CAD 系统与快速原型制造系统之间的数据交换接口。该切片算法已在“超人 2000 CAD/CAM”系统中实现,算法表现稳定。

关 键 词:计算机辅助设计;快速原型制造;STL 文件

中图分类号:TP301

文献标识码:A

Application of NURBS in RPM Systems

ZHUANG Hai-jun, ZHOU Ru-rong, TANG Jie, ZHANG Li-yan, ZHOU Lai-shui

(CAD/CAM Engineering Research Center, Nanjing University of Aeronautics and Astronautics, Nanjing 210016)

Abstract: STL file is used as the data interface between most of the RPM systems and CAD system. However, STL file is created by drawing up part surface with a series of triangle patches, which may cause some problems. Although increasing the number of triangle patches and decreasing the dimension can improve the precision, the STL files is made too bigger and post process time much longer at the same time. This paper aims to resolve these constrictions by presenting a data exchange method between CAD system and RPM system. The data of RPM system is obtained directly from the slicing data of the model in CAD system. The algorithm has been implemented in the "Superman 2000 CAD/CAM" software. Applications show that the algorithm is stable and efficient.

Key words: NURBS(Non-Uniform Rational B-Spline); Computer aided design; Rapid prototyping manufacturing (RPM); STL(Stereolithography) file

快速成型(Rapid Prototyping Manufacturing)技术是基于离散/堆积成型的原理,具有极高柔性的新的制造技术,是 80 年代后期发展起来的一项新的制造技术。快速成型技术直接利用 CAD 所生成的数据,在计算机控制下,使材料快速成型为三维实体模型 STL 文件作为 CAD 系统与快速原型系统之间的数据交换接口已经得到广泛的认可。它是在给定精度要求下,用一系列的三角片逼近实际曲面而产生的。在快速原型系统对三角片进行切片,填充处理,计算出激光头的位置信息,送至快速原型机的控制系统,完成零件的加工。

但是,用 STL 文件作为 CAD 系统与 RPM 系统之间

的数据交换接口也存在一些不足之处。用户在 CAD 系统中构造的精确模型必须离散成用一系列三角片表示的模型才能输入到 RPM 系统中。增加三角片的数量可以提高模型离散的精度,但同时增大了数据文件,延长了切片和填充处理时间。而且,STL 文件本身及其创建过程均存在许多缺陷^[1]。这些缺陷给后续处理带来不便,甚至引起灾难性的结果。目前,许多研究人员正在致力于改进 CAD 系统与 RPM 系统的数据交换接口^[2,3]。

本文分析了 STL 文件作为 CAD 系统与快速原型系统之间的数据交换接口的缺陷和不足,提出一种 CAD 系统与 RPM 系统之间新的数据交换方法。该方法对 CAD 系统中的真实模型直接切片,将切片后所得到的轮廓数据作为 CAD 系统与快速原型制造系统之间的数据交换接口。该切片算法已在“超人 2000 CAD/CAM”系统中实现,算法表现稳定。

收稿日期:2001-06-27

基金项目:国家重点科技攻关专题“面向制造业 CAD/CAM 系列软件开发及商品化”(96-A01-01-05)和江苏省九五攻关项目“计算机辅助数控及加工仿真系统”(G98017-3)资助

作者简介:庄海军(1970-),男(汉),河北,博士研究生

E-mail:hj-zhuang@zaobao.com

1 STL 文件的缺陷

快速原型制造的切片过程如图 1 所示。用户在 CAD 系统中设计好模型后,对其三角化,输出 STL 文件,再输入到 RPM 系统。在 RPM 系统中,每个三角片与平行于 XOY 平面的无限平面求交,具有相同 Z 坐标的交线段连接起来就成为该层的轮廓。然后对每层轮廓填充,求得激光头的扫描轨迹。CAD 系统与快速原型系统之间的数据交换接口在快速原型技术中占有非常重要的地位。目前最常见的数据交换格式是 STL 文件格式(StereoLithography file)。它是由 3D Systems 公司在 1987 年首先提出的。当今大多数 CAD 系统,如 UG-Ⅱ, AutoCad 等,都有 STL 文件生成模块。实际上,STL 文件已经成为 CAD 系统与快速原型系统之间数据交换的不成文的标准。STL 文件格式如图 2 所示。

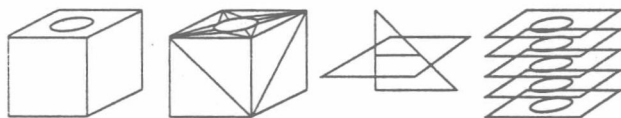


图 1 快速原型系统切片过程

Solid			
facet normal	0.000000	0.000000	-1.000000
outer loop			
vertex	60.838149	55.366549	13.219109
vertex	58.457196	55.366549	13.219109
vertex	60.838149	52.985597	13.219109
endloop			
endfacet			
⋮			
endsolid			

图 2 STL 文件格式

STL 文件格式最初用于立体光造型技术(SLA)。由于 STL 文件简单易读,又与具体的 CAD 系统无关,因而很快发展成为快速原型领域中 CAD 系统与快速成型机之间不成文的数据交换标准。但是,STL 文件一出现,研究人员就发现它存在严重的不足:

(1) STL 文件存在严重的数据冗余。在对 CAD 模型三角化时,为提高模型的精度,必须采用很细小的三角片,这就造成 STL 文件庞大,分层切片处理时间延长。同时,三角片过小还会导致零件表面形状失真。这是由于当三角片的某条边过小时,分层处理软件会将其作为一点来处理,造成三角片丢失。

(2) 带有缺陷的 STL 文件。现有的 CAD 系统在处理较为复杂的零件时,三角化的结果存在一些缺陷。如裂缝、重叠等现象(如图 3 所示),这些缺陷会给后续处理带来不便甚至是灾难性的结果。

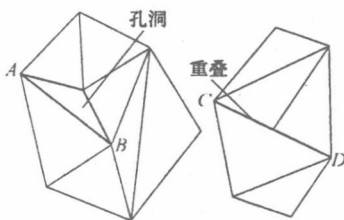


图 3 三角化的结果的缺陷

2 真实模型直接切片法

从前述快速原型制造的切片过程可以看出,由 STL 文件切片而得到的模型,其精度不可能高于 STL 文件对真实模型的逼近精度。通过增加三角片的数量来提高模型离散的精度,必然会增大 STL 数据文件,延长切片和填充处理时间,同时还会增大三角片缺陷出现的机率。显然,获得高精度模型的最好的办法是直接对真实模型切片。目前,许多 CAD 系统均采用精确实体来表示复杂零件,基于实体的求交算法也较为成熟,其交线是一 NURBS 曲线, NURBS 曲线是建立在 B 样条的基础上,既保留了其描述自由曲线的长处,又具有精确表示二次曲线的能力,因此 NURBS 曲线可以统一表示所有曲线。一条 P 次 NURBS 曲线的数学表达式为

$$c(u) = \frac{\sum_{i=0}^n N_{i,p}(u) W_i P_i}{\sum_{i=0}^n N_{i,p}(u) W_i} \quad (1)$$

式中: P_i 为控制顶点; W_i 为控制顶点 P_i 的权因子; $N_{i,p}(u)$ 为 P 次规范 B 样条基函数。采用递归定义为

$$N_{i,0}(u) = \begin{cases} 1 & u_i \leq u \leq u_{i+1} \\ 0 & \text{其他} \end{cases}$$

$$N_{i,p}(u) = \frac{u - u_i}{u_{i+p} - u_i} N_{i,p-1}(u) + \frac{u_{i+p+1} - u}{u_{i+p+1} - u_{i+1}} N_{i+1,p-1}(u)$$

“超人 2000 CAD/CAM”系统是基于一 ACIS 几何平台的新一代 CAD/CAM 系统, ACIS 是美国 Spatial Technology 公司推出的面向对象的三维几何造型平台,它集线框、曲面和实体造型于一体,并允许这三种表示共存于统一的数据结构中。ACIS 的求交算法已经相当高效和稳定,且求交精度可达 10^{-8} mm,完全满足工程设计的要求,作者在“超人 2000 CAD/CAM”系统上开发了对真实模型直接切片的算法。从模型的 Z_{\min} 到 Z_{\max} ,步长为 step,对每一个平行于 XOY 平面的无限平面,与真实模型求交。交线为由一组 NURBS 曲线组成的切片轮廓。这些 NURBS 曲线即可输出到文件,以备快速原型制造系统应用。

3 NURBS 曲线的离散

经过对真实模型的直接切片处理,我们得到了以 NURBS 曲线表示的切片轮廓。但是,快速原型制造系统目前接受的是以连续折线段表示的切片轮廓,因而,必须将所得的 NURBS 曲线离散成连续折线段。

NURBS 曲线轮廓的离散应按照以下两个准则:离散要满足一定的精度;应产生尽量少的折线段,以减少填充时间。

4 容差离散法

如图 4 所示,在本文中,容差 t 定义为曲线到折线段的最大距离。

为加快算法的处理速度,本文采用了一些近似算法。对于图 4 所示的折线段,我们以参数域上的中点所对应的弦高为容差。显然,这会引起误差,但当折线段较小时,已经足

够了。为了减小近似算法的影响, 我们还将用户指定的精度乘以一定的系数, 一般取 0.8。

离散算法的具体描述如下:

- (1) 读入一条 NURBS 曲线;
- (2) 检查该 NURBS 曲线是否是直线, 如是, 则直接送到轮廓数据结构, 返回 1;
- (3) 取 U_1 = 该 NURBS 曲线参数域的下界, $U_2 = U_1 + \text{step}$. step 为步长, 一般取 0.05;
- (4) 计算 $U_1 U_2$ 折线段对应的容差 t ;
- (5) 如容差 t 大于精度 ϵ , 取 $U_1 = U_1, U_2 = (U_1 + U_2) / 2$, 返回 4;
- (6) 如容差 t 小于精度 ϵ , 取 $U_1 = U_2, U_2 = U_1 + \text{step}$, 返回 4;
- (7) 如 U_1 大于该曲线参数域上界, 返回 1;
- (8) 直到所有 NURBS 曲线均处理完毕。

至此, 得到了离散后的模型的轮廓, 可以对其进行填充处理, 生成激光头的扫描数据了。

5 应用

作者以直径为 50 mm 的小球为例来进行比较。加工精度分为粗、中、精三等, 粗等容差为 0.1, 中等容差为 0.05, 精等容差为 0.001。分别用 STL 文件和本文提出的切片轮廓作为 CAD 系统与快速原型系统之间的数据交换接口。切片轮廓以“超人 2000 CAD/CAM”系统的数据文件 SMF 存储。比较结果如表 1 所示: (单位: Kbytes)

表 1 SEL 文件与直接切片的比较

	粗	中	精
STL 文件	48.5	150.2	298.4
直接切片	60.3	72.1	75.2

由表 1 可以看出, 真实模型直接切片法与 STL 文件相比, 具有明显的优越性。

6 结束语

本文分析了 STL 文件作为 CAD 系统与快速原型系统之间的数据交换接口的缺陷和不足, 提出一种 CAD 系统与 RPM 系统之间新的数据交换方法。该方法克服了 STL 文件的不足, 具有高效、稳定、简单等优点。

[参考文献]

[1] Roscoe L E, Chalasani K L, Meyer T D. Living with STL files[A]. Proceedings of the 6th International Conference on

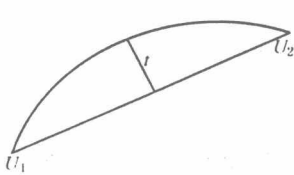


图 4 容差的定义

Rapid Prototyping[C]. Dayton. Ohio. U.S.A, 1995

[2] Chua C K, Gan G K J, Tong Mei. Interface between CAD and rapid prototyping systems. Part 1: A study of existing interface[J]. Int. J. Adv. Manuf Technol. 1997.13:566~570

[3] Chua Chee Kai, Gan G K, Jacob, Tong Mei. Interface between CAD and rapid prototyping systems. Part 2: LMI-An improved interface[J]. Int. J. Adv. Manuf Technol, 1997. 13:571~576

[4] 施法中. 计算机辅助几何设计与非均匀有理 B 样条 (CAGD&NURBS)[M]. 北京航空航天大学出版社, 1994

(上接第 994 页)

3 结束语

在协同产品开发过程中, 由于每位人员都有自己的语言和背景知识, 因此知识的交流和共享是基础和瓶颈问题, 同时也是部分冲突产生的根源。本体论通过规范化定义领域内词汇及其意义的方式在语义级上解决了上述的部分问题。然而当前各种本体表示方式没有严格描述概念本质的方法。本文提出了 TONE 本体模型, 通过严格区分术语的内涵和外延, 提出绝对化属差, 建立了概念内涵二叉树, 使概念内涵的定义明确化和清晰化; 建立了内涵向外延构造的基本算子, 使本体中的基本元素-术语-的意义得到统一成为可能, 为知识的交流和共享提供了支持。

[参考文献]

[1] Gruber T R. Ontolingua: A Mechanism to Support Portable Ontologies[R]. KSL-91-66, Knowledge Systems Laboratory, Stanford University. November, 1992

[2] Genesereth M R, Fikes R E. Knowledge Interchange Format, Version 3.0 Reference Manual [R]. KSL-91-66, Knowledge Systems Laboratory, Stanford University. 1992.6

[3] Brachman R, Borgida A, McGuinness D. The classic knowledge representation system[A]. In: Proc of Intl Conf on 5th Generation Systems[C]. Tokyo, 1992



ELSEVIER

Journal of Materials Processing Technology 129 (2002) 261–267

Journal of
**Materials
Processing
Technology**

www.elsevier.com/locate/jmatprotec

Classification and analysis of tube hydroforming processes with respect to adaptive FEM simulations

L. Gao^{a,*}, S. Motsch^b, M. Strano^c

^aCollege of Mechanical and Electrical Engineering, Nanjing University of Aeronautics and Astronautics, Nanjing 210016, PR China

^bMTU Berlin-Brandenburg Aero Engines GmbH, Entwicklung Rotormechanik MLE, Adolf-Rohrbach-Str.10 D 14974, Ludwigsfelde, Germany

^cDipartimento di Ingegneria Industriale, Università di Cassino, via di Biasio 43, 03043 Cassino (FR), Italy

Abstract

A classification of tube hydroforming (THF) processes based on sensitivity to loading parameters has been suggested. The characteristics of the classification have been analyzed in terms of failure mode, dominant loading parameters and their working windows. It is considered that the so-called pressure dominant THF process is the most difficult process for both simulation in FEM analysis and practical operation in real manufacturing situation. To effectively determine out the optimum loading path for pressure dominant THF process, adaptive FEM simulation strategies are mostly needed.

© 2002 Elsevier Science B.V. All rights reserved.

Keywords: Tube hydroforming; Process classification; Loading path; Adaptive simulation

1. Introduction

Tube hydroforming (THF) is a relatively new technology which has enjoyed increasingly widespread application in industry. Due to the complicated nature of plastic deformation of THF, FEM analysis is used widely to simulate the process in order to shorten the development time and reduce prototyping cost [1]. Of all the parameters in both FEM simulation and practical process control, the most important ones are the so-called loading path parameters which includes both the internal pressure and the axial feeding [2,3]. The relationship of these parameters with time are called the loading path. Compared with the stamping process where the loading parameter is mainly the punch velocity or displacement, THF processes are more difficult to simulate and to control. In most cases, the loading path of THF processes are determined on a trial-and-error basis and hence the simulation can be quite time consuming. In order to reduce the lead time for THF process planning, ideas of adaptive simulation has been suggested [4,5]. It is expected that by pre-setting some control parameters and selecting some strategies to automatically adjust the loading parameters during the simulation, a relatively good loading path, which will ensure a good part free of both wrinkles and excessive thinning, could be found in a single simulation

run. Parts which can be formed by THF are numerous and are quite different in shapes. On one hand, it is very difficult to find a general procedure such as a universally applicable wrinkle indicator, leaking indicator, and so on in adaptive simulation, and on the other hand, due to quite different sensitivity to the loading parameters, the need for adaptive simulation and the strategies to effectively simulate the specific process may vary greatly.

This paper is devoted to classify and briefly analyze THF processes based on their sensitivity to the loading parameters, in a belief that this classification will enable FEM simulation in general and adaptive simulation in particular to be used effectively where it is mostly needed.

2. Idea of a THF processes classification based on sensitivity to loading parameters

THF processes have been classified basically according to geometries or failure modes of the parts [6,7]. The suggested classification in this paper, however, is based on the process sensitivity to loading parameters. Since these parameters have a decisive role in the failure modes, i.e. fracture is mainly related to excessive pressurization and wrinkling is mainly related to excessive axial feeding, a classification based on sensitivity to loading parameters will roughly tell, among other things, the working windows or margins of each loading parameter in which a good part can be made.

* Corresponding author. Tel.: +86-25-4892508; fax: +86-25-4891501.
E-mail address: lingao@cnuninet.com (L. Gao).

Axial force may also be used as a loading parameter, but in cases where wrinkles are likely to occur, the axial force is not related monotonously to the feeding displacement. Once a wrinkle sets in, the tube resistance to punch movement is lost substantially, resulting a rapid movement of the punch at a decreasing axial force [8]. In other words, for the same known axial force, the exact amount of axial feeding may not be known. The amount of axial feeding is considered more closely related to the overall deformation and thus it is considered an important loading parameter to be controlled.

Generally speaking, THF processes, according to their sensitivity to axial feeding and internal pressurization, can be divided into four groups: (1) pressure driven THF; (2) pressure dominant THF; (3) feeding dominant THF and (4) feeding driven THF. Examples with brief analysis will be given to describe each group. This classification is a basic classification, which means that there can be a certain part having portions belonging to different categories of this classification. However, if the basic characteristics of each category are understood, we might be in a better position to handle both the simulation and the practical THF process control.

3. Case A: pressure driven THF process

THF processes that do not need feeding (a small bulging ratio) or can be fed very little (a part with too many bendings, protrusions, etc. along the tube) fall into this category (engine cradle may be one example). Then the two loading parameters are reduced almost to one. Since there is no or little feeding, there is basically little risk of wrinkling in this group. However, the risk of leaking could be high, especially in the case of zero feeding, due to relatively large axial tensile stress trying to pull the tube away from the sealing punch. This can also be seen clearly in THF simulations as a self-feeding phenomenon. In the extreme case when the punch does not move, the punch has to sustain a tensile axial stress to keep the tube from self-feeding. The magnitude of

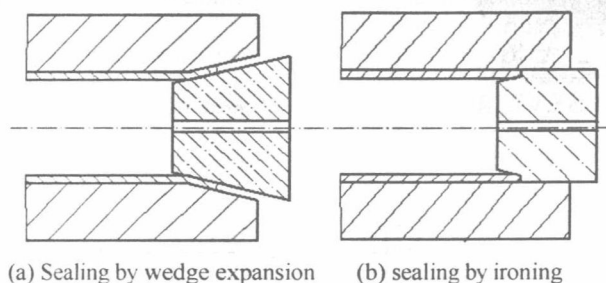


Fig. 1. Sealing mechanism.

the stress is about half of the hoop stress and is at its maximum when the tube start to bulge (when there is no feeding, the stress state in the elements starting to bulge is close to the plane-strain state). The major problem to handle for this group of THF processes is to maintain a good sealing. This can be achieved by the application of an edge expansion sealing mechanism (Fig. 1(a)) when there is no need for feeding or by ironing sealing mechanism (Fig. 1(b)) when small feeding is needed and possible [9].

For cold THF processes, metals have little strain-rate sensitivity. Thus, in simulation of the THF process in this group by using a dynamic FEM code, if the deformation rate is reasonably low, as suggested in the user's manual to avoid impact effects, the pressure versus time curve is very easy to select. The underlying meaning is that the amount of deformation is mainly related to the final pressure level. How the pressure level is reached is of little significance (as long as the material is not too strain-rate sensitive and the load is not increased so quickly as to cause an impact effect). In other words, if one does not apply sufficient pressure, one simply does not reach the necessary amount of deformation. Then the only failure mode for this group is fracture, which depends mainly on material-related parameters such as tube formability, tube thickness, tube diameter, friction condition, pre-form shape, welding quality, etc., while relying little on the loading path. To illustrate this, a simple symmetrical

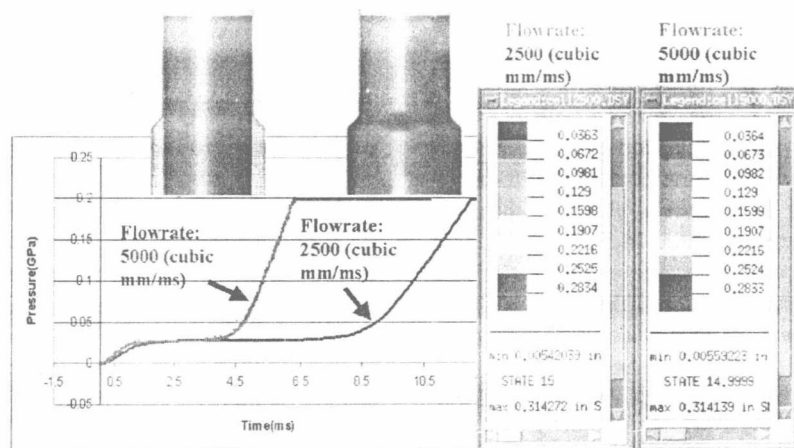


Fig. 2. Comparison of simulation results of flow rate effect.

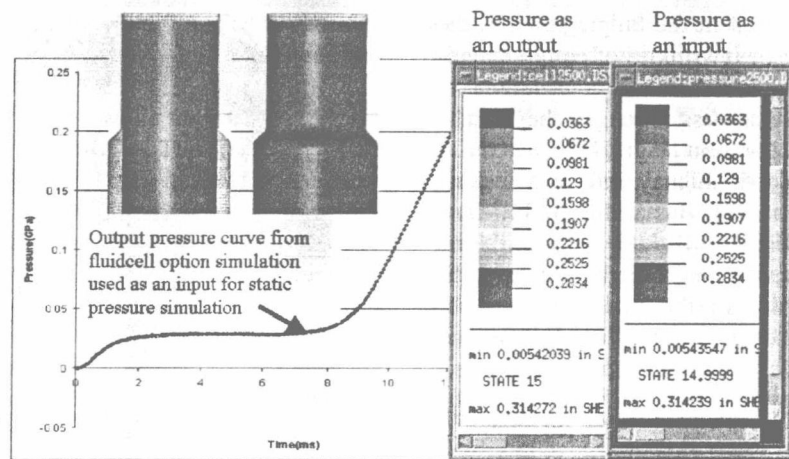


Fig. 3. Comparison of simulation results between fluid cell option and static pressure option.

bulging of a low carbon steel (1008) tube is simulated (Figs. 2 and 3). The expansion ratio is relatively small (25%) to allow an acceptable maximum thinning without feeding. First a fluid cell option is used in simulation. Flow rate starts from 0 and then linearly reaches a constant value in 1 ms. (Note that in order to save cpu time, in PAMSTAMP simulation, a time scale factor of about 1000 is commonly used so that 1 ms is about 1 s in the real case. At the same time, attention should be paid to make sure that tooling speed does not exceed the limit suggested in the FEM code manual.) The maximum pressure is set to be 200 MPa to calibrate the corner. Fig. 2 shows that as long as the final pressure is the same, the rate to reach that pressure has little effect on the maximum thinning and the thinning range. Fig. 3 shows that for the same THF part, if the output pressure versus time curve is used, obtained from a fluid cell option simulation as a input pressure versus time curve in a static pressure option simulation, then the latter simulation will be almost identical with the former simulation. This is of great help in finding a pressure curve that ensures a smooth deformation. What may be done is to set a limit pressure for the process and select a constant flow rate for the simulation. The resultant pressure versus time curve could be the ideal loading path to control a smooth bulging for making good THF parts of this group. The loading path is relatively easy to determine for THF of this group, therefore, there is no need to rely on adaptive simulation to find a relatively good loading path. In case of having fracture, then such things as modifying the tooling design, selecting a new blank tube with better formability or optimizing the shape of the preform have to be worked on.

4. Case B: pressure dominant THF process

Parts in this group have an expansion ratio larger than those in the first group, so more axial feeding is essential for the successful bulging of the parts. Once large feeding is

involved, there will be a new risk of wrinkling or buckling. On the other hand, due to the nature of a relatively large expansion ratio, the deformation may exceed the pressure instability point. Starting from this point, a drastic expansion sets in without increase in the internal pressure, hence the risk of fracture runs high [10]. What is more, the drastic expansion may generate a rapid pulling movement at the tube end, resulting another problem: leaking. Although parts in this group often look simple (most parts have a large degree of symmetry and a relatively large expansion area), they are in reality among the most difficult parts to be formed successfully in both simulation and in reality, for the aforementioned reasons. Fig. 4 shows typical failed parts with a straight central line. Failures are shown as large wrinkle (too much feeding relative to the pressurization) or as excessive thinning (pressure too high relative to the amount of axial feeding).

Of the two loading parameters, pressure is more important than feeding for THF of parts in this group, because

- (1) Most bulging deformation is achieved by pressurization, while feeding may also help to form the part by

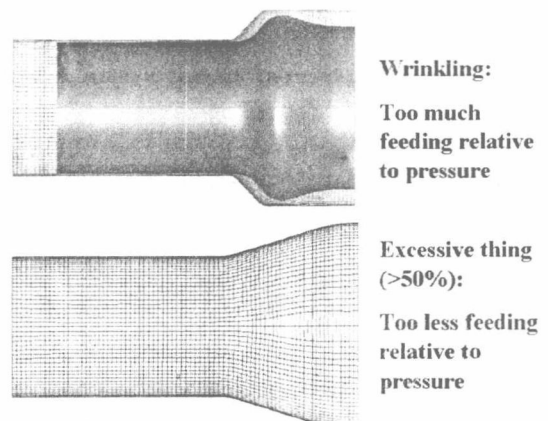


Fig. 4. Two failure modes in a symmetrical bulged part.

accumulating more material in the bulging area in the form of removable wrinkles (wrinkles of proper magnitude in this group are often considered as beneficial to the successfulness of the process as long as they can be removed in the final calibration stage [11]).

- (2) The drastic expansion (which may induce a leaking problem) after the pressure instability point is a important issue to handle.
- (3) High pressure often has to be applied to remove the “good” wrinkles created in the early stage of the process and calibrate the part to its required dimension and geometry.

Another characteristic of this process is the so called self-feeding phenomenon. In ERC/NSM of The Ohio State University, static pressure is applied in the first trial simulation only to the internal surface of the tube (this generally cannot happen in reality except when applying a sliding sealing punch which allows a relative movement of the tube from the sealing punch). Further assuming zero friction, an obvious self-feeding can be observed. The amount of self-feeding could be the starting point of how much feeding is needed. When large thinning is observed in the first trial self-feeding simulation, additional feeding usually has to be applied in the real simulation in order to accumulate enough material in the bulging area to successfully form the part.

Another example of this group is the bulging of a prebent tube with a curved central line. It is very easy to get wrinkling, excessive thinning or both. The part material (Fig. 5) is a stainless steel ss409. No matter how the feeding distance is changed, excessive thinning is inevitable. Excessive thinning in point A is due to relatively small feeding while excessive thinning in the inner bending radius area (point B in Fig. 5) is due to too large feeding. In fact, fracture in area B is wrinkling induced, which means that once a wrinkle starts to grow around point B, it would need an extremely larger pressure to push the valley area of the wrinkle outward to be flattened and this effort would only make the thickness in the valley area even greater and the thickness in the peak area to be even less. The result is: before one could eliminate the wrinkle, the peak area of the wrinkle will burst while the valley area is still not flattened. One alternative method other than trying hard to find a optimized loading curve from among a narrow working

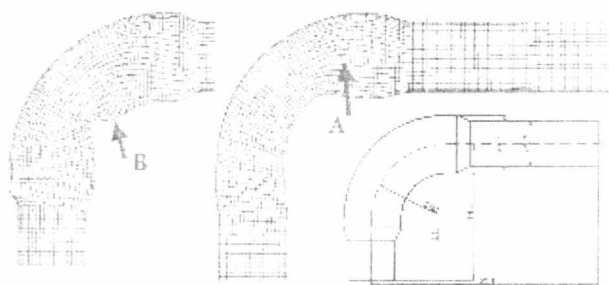


Fig. 5. Failure modes in bulged parts made from prebended tubes.

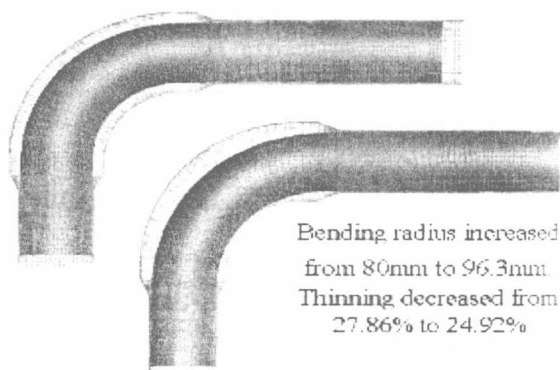


Fig. 6. Prebending radius increased to reduce risk of thinning and wrinkle.

window is simply to change the bending radius within the cavity boundary of the hydroforming die (Fig. 6). This change will make the prebent tube less work hardened and allow more feeding without wrinkling in the following hydroforming process, thus bringing the thinning down from 27.87 to 24.92% in the case of ss304 material.

Since the THF process of this group has the most failure modes (fracture, wrinkle, leaking), whilst the working margin of the loading parameters that one can play with are often narrow, simulation of such a process will undoubtedly involve a lot of trial-and-error. Therefore, this is the area where adaptive simulation is mostly needed. Only in the case where a practical loading path to form a good part does not exist, does one have to redesign the part or the preformed tube. To better apply the adaptive simulation concept in THF processes simulation of this group, the following issues need to be clarified.

4.1. The wrinkle indicator

Wrinkles occurring in THF processes of this group should be allowed in a controlled manner. The basic criterion as to whether a wrinkle is useful or not is judged by the simple fact as to whether it can be finally smoothed out by the calibration pressure available. Thus the need for a sensitive wrinkle indicator is relaxed while a good timing which could be coupled with the wrinkle indicator to stop feeding and start calibration is needed to remove the wrinkles confined by the preset wrinkle indicator.

4.2. Loading strategy

Time (as in the relationship of pressure versus time and axial feeding versus time) in simulation is only an intermediate variable which has little meaning if the material is not very strain-rate sensitive and the tooling speed selected is kept below the limit suggested by the FEM software developer. The fundamental loading path that determines the outcome of the process is the pressure versus axial feeding curve. Hence, of the two loading parameters, one can be fixed as linear or rectilinear and only the other changed to